AD-A115 387 FOREIGN TECHNOLOGY DIV WRIGHT-PATTERSON AFB OH F/G 20/4
THE NUMERICAL SOLUTION OF MACH-ZEHNDER INTERFEROGRAM ANALYSIS O--ETC(U)
APR 82 P DING, S PAN
UNCLASSIFIED FTD-ID(RS)T-0016-82 NL

END
DATE FILMED
7 82
DTIC

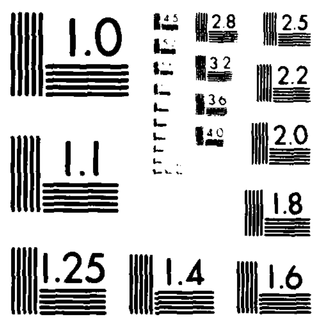

MICROCOPY RESOLUTION TEST CHART

NATIONAL BUREAU OF STANDARDS-1963-A

FTD-ID(RS)T-0016-82

FOREIGN TECHNOLOGY DIVISION

AIR FORCE SYSTEMS COMMAND

THE NUMERICAL SOLUTION OF MACH-ZEHNDER INTERFEROGRAM ANALYSIS OF SUPERSONIC AIRFLOW ABOUT CYLINDRICAL AND SYMMETRICAL PROJECTILES

by

Ding Peizhu and Pan Shoufu

FOREIGN TECHNOLOGY DIVISION

FTD-ID(RS)T-0016-82

EDITED TRANSLATION

FTD-ID(RS)T-0016-82 28 April 1982

MICROFICHE NR: FTD-82-C-000524L

THE NUMERICAL SOLUTION OF MACH-ZEHNDER INTERFEROGRAM ANALYSIS OF SUPERSONIC AIRFLOW ABOUT CYLINDRICAL AND SYMMETRICAL PROJECTILES

By: Ding Peizhu and Pan Shoufu

English pages: 16

Source: Acta Scientiarum Naturalium Universitatis Julinensis, Nr. 3, 1981, pp. 60-71

Country of origin: China
Translated by: LEO KANNER ASSOCIATES
F33657-81-D-0264
Requester: FTD/TQTA
Approved for public release; distribution unlimited.

GRAPHICS DISCLAIMER

All figures, graphics, tables, equations, etc. merged into this translation were extracted from the best quality copy available.

THE NUMERICAL SOLUTION OF MACH-ZEHNDER INTERFEROGRAM ANALYSIS OF SUPERSONIC AIRFLOW ABOUT CYLINDRICAL AND SYMMETRICAL PROJECTILES

Ding Peizhu and Pan Shoufu

SUMMARY:

In this study, four physical conclusions and the numerical solutions described in [1] concerning the Abel transformation in Plasma Spectroscopy involving shock-waves extended to the Mach-Zehnder interferogram analysis in supersonic airflow about cylindrical symmetrical projectiles. Regarding the relation between the interferometric fringe shift $\delta(x,z)$ and the concentration variation $\rho(r,z)-\rho_0$ obtained at each point of the supersonic airflow field, we obtained three physical conclusions similar to those described in [1]. In addition we provided the interferometric fringe shift $\delta(x,z)$ obtained from observations and the coefficient formulas of the entire transformation necessary to calculate the concentration variation $\rho(r,z)-\rho_0$ at every point of the airflow field.

We borrowed from source [2] the airflow field density computation method provided for the Mach-Zehnder interferogram applied to supersonic symmetrical projectiles, and obtained satisfactory results. Also, a simplified method for computation is given for the case of additional shock-waves present in the airflow field.

I. INTRODUCTION

The question of the airflow about supersonic cylindrical symmetrical projectiles is old and of sizeable importance. The Mach-Zehnder interferogram analysis (*) has been for many years an important and practical research tool. Since the invention of digital computers, extensive applications occurred in the M-Z interferogram analysis. The method of interferogram analysis consists in measurements of the interferometric fringe shift $\delta(x,z)$, the research of the concentration variations $\rho(r,z)-\rho_0$ at every point of the airflow, using the Abel transformation; thereby we obtained the curve of density in plasma spectroscopy.

(*) below: "M-Z interferogram" or "interferogram".

In the past scientists have applied the integral of Stieljes to obtain numerical solutions of the above problem [3]. But experimenters are still not familiar with the application of the numerical solutions of the integral of Stieljes; further, the results computed thereby present some ambiguities in this case of shock-waves. In [1], we discussed some characteristics relative to the usual simplified solution of the Abel equation. By using the Abel equation with a radiation frequency I(x) in plasma spectroscopy involving shock-waves and an emission coefficient (E(r), we demonstrated that E(r) can be computed from the usual Abel transformation, and we obtained the formula E(r) for the computation of the amplitude of the shock-waves.

This is why we suggested in [1] a new computation of the Abel transformation in plasma spectroscopy involving shock-waves.

In the M-Z interferogram analysis, equations noted as $\delta(x)$ and $\rho(r)-\rho_0$, the radiation frequency in plasma spectroscopy I(x), and the emission coefficient E(r) are mathematically identical. Therefore it is possible to extend directly the conclusions and methods of computation obtained in [1], to the Abel transformation of interferogram analysis about cylindrical and symmetrical supersonic projectiles. The method of computation is simple. The physical theory applied to the shock-waves is equally understandable.

In the second part of this study, we describe the Abel transformation of interferogram analysis about cylindrical, symmetrical supersonic projectiles. In addition, we extended the conclusions obtained in [1] concerning the Abel transformation in plasma spectroscopy involving shock-waves to the present case. In the third part we have listed numerical solutions. In the fourth part we discuss the case of an additional shock-wave. The fifth part is a possible plan for a simplified computation in the case of an additional shock-wave.

II. THE ABEL TRANSFORMATION

Figure 1 illustrates a point-headed supersonic projectile in flight.

We suppose that conditions are such as: it is cylindrical and symmetrical, and that there are one or several tapering shock-waves moving towards the back. Section 1-1 is illustrated on Fig. 2: the hatched circle in the center represents the cross section of the projectile; the circumference c represents the cross section of the shock-wave. Outside c, the airflow has not yet been affected by the wave's interference. The density and the index of refraction are respectively ρ_0 and n_0; within c, since we are dealing with a cylindrical, symmetrical projectile, the density and the index of refraction only reach the distance r related to the center 0, and are respectively:

$$\rho=\rho(r), \qquad n=n(r)$$

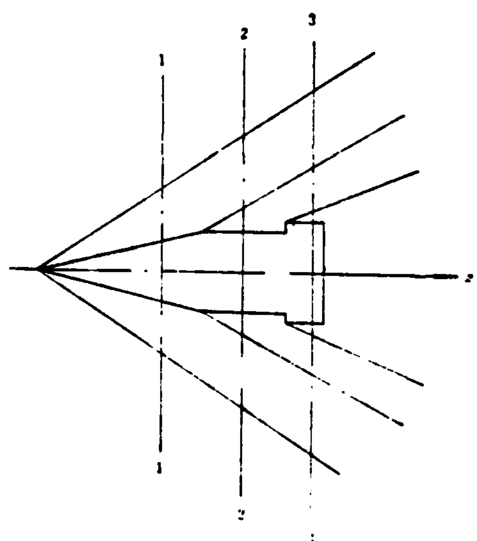

Fig. 1. Illustration of the cylindrical, symmetrical supersonic projectile in flight.

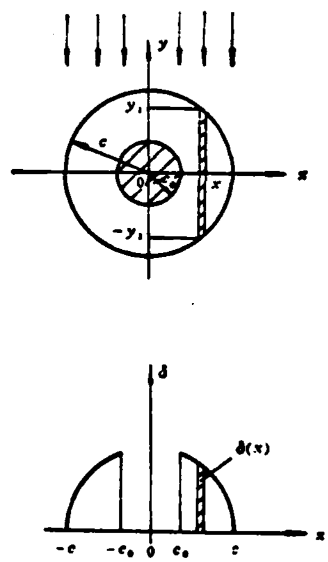

Fig. 2. Illustration of photoline according to cross-section 1-1.

Fig. 2 illustrates the interferometric fringe shift corresponding to section 1-1. The value $\delta(x)$ at point x is the light crossing section 1-1 refracting the superimposed effect of one beam going from -y to y_1 and away from the y axis for each value of x.

According to the usual hypothesis, the interferometric fringe shift $\delta(x)$ and the refraction index difference $n(r)-n_o$ or the density difference $\rho(r)-\rho_o$ satisfies the equation: (*)

$$\delta(x) = \frac{1}{\lambda^*}\int_{-y_1}^{y_1}(n(r)-n_0)dy \doteq \frac{K}{\lambda^*}\int_{-y_1}^{y_1}(\rho(r)-\rho_0)dy,$$

in which K is the Gladstone-Dale constant, λ^* is the wave length in monochromatic light and total vacuum necessary for obtaining the interferogram. Focusing on the cylindrical characteristics and the value of $x^2+y^2=r^2$, the above equation becomes:

$$\delta(x) = \frac{2K}{\lambda^*}\int_x^c \frac{(\rho(r)-\rho_0)r}{\sqrt{r^2-x^2}}dr. \qquad (1)$$

We assume that the shock-wave is a simplification of the first category of $\rho(r)-\rho_o$ (or $n(r)-n_o$). If c is the most external shock-wave, then outside c, $\rho(r)-\rho_o=0$. And therefore Eq. (1) can be written:

$$\delta(x) = \frac{2K}{\lambda^*}\int_x^R \frac{(\rho(r)-\rho_0)r}{\sqrt{r^2-x^2}}dr, \qquad (2)$$

in which R is an arbitrary constant superior to c. Besides the constant $2K/\lambda^*$, Eq. (2) and the Abel equation encountered in the study of plasma spectroscopy involving shock-waves are similar. Bennett and his colleagues have studied Eq. (2) in [2]; in [1] we discussed some characteristics of the solution of the Abel equation. If we apply them to Eq. (2), we obtain:

1) on the M-Z interferogram's arbitrary cross section 1-1, the fringe shift is continuous.
2) If, on section 1-1, the shock-wave c belongs to the first category interrupted $\rho(r)$ and $\rho'(r)$, then inside the shock-wave we have:

$$\delta'(x) = \frac{2Kx}{\lambda^*}\int_x^R \frac{\rho'(r)}{\sqrt{r^2-x^2}}dr + \frac{2Kx}{\lambda^*}\frac{\rho(c_+)-\rho(c_-)}{\sqrt{c^2-x^2}}, \qquad (3)$$

especially when $x \to c$.

$$\delta'(x) \sim \frac{K\sqrt{2c}}{\lambda^*}\frac{\rho(c_+)-\rho(c_-)}{\sqrt{c-x}}, \qquad (4)$$

(*) See [2].

3) If the fringe shift is smooth outside the peaks c, then $\lim_{x\to c_+} \delta'(x)$ exists; when $x\to c$, $\delta'(x) \sim L/\sqrt{c-x}$, then shock-waves appear outside the airflow circle r=c, on the cross section 1-1; the density saltatory value of the shock-waves will be

$$\rho(c_-) - \rho(c_+) = -\frac{\lambda^* L}{K\sqrt{2c}}, \tag{5}$$

further, on $[c_0, c]$ and $[c, R]$

$$\rho(r) - \rho_0 = -\frac{\lambda^*}{\pi K}\int_r^R \frac{\delta'(x)}{\sqrt{x^2 - r^2}}\,dx. \tag{6}$$

These conclusions are also applicable in the case of a single shock-wave.

III. NUMERICAL SOLUTIONS

We will first discuss the case of c with a single shock-wave. For a convenient application to the case of several shock-waves, "The $\rho(r)-\rho_0=0$ external to c" is transformed into: "on $[c,R]$, $\rho(r)$ and $\rho'(r)$ are continuous when $r\geq R$, $\rho(r)-\rho_0=0$." Evidently, the former is a particular of the latter.

With $[0,R]N$, we have the following partition:

$$o = x_0 < x_1 < \cdots < c = x_\nu < x_{\nu+1} < \cdots < x_N = R$$

or

$$o = x_0 < \cdots < c_0 = x_\mu < x_{\mu+1} < \cdots < x_\nu = c < x_{\nu+1} < \cdots < x_N = R.$$

We also note: $h = x_{k+1} - x_k, \delta_k = \delta(x_k)$. According to conclusion 2 obtained in section II, the derivative $\delta'(x)$ of the interferometric fringe shift tends toward the moment of the shock-wave with the value $1/\sqrt{c-x}$ and toward the infinite from inside the shock-wave. Consequently, one more term is used in the expression of the shock-wave, $1/\sqrt{c^2-x^2}$, for the breakdown of the comparable $\delta(x)$. On $[x_{\nu-2}, c]$ and $[x_{\nu-1}, c]$ we extract

$$P_{\nu-2}(x) = P_{\nu-1}(x) = \bar{a} + \bar{b}x + \bar{c}x^2 + l\sqrt{c^2 - x^2} \tag{7}$$

the comparable, $\delta(x)$, zero.

We can state $P_{v-2}(x_k) = P_{v-1}(x_k) = \delta_k, \quad k = v-3, v-2, v-1, v,$

including $\bar{a}$, $\bar{b}$, $\bar{c}$, $l = \frac{1}{Dh}\left\{-\delta_v + 3\delta_{v-1} - 3\delta_{v-2} + \delta_{v-3}\right\}$ (8)

Then extracting from $D = 3\sqrt{2v-1} - 3\sqrt{4v-4} + \sqrt{6v-9}$.

$$[x_j, x_{j+1}]\,(j = w+1, w+2, \cdots, v-3)$$

$$P_j(x) = a_j + b_j x + c_j x^2 + d_j x^3 + l\sqrt{c^2 - x^2},$$

When $c_0 \geq 0$, we extract from $[c_o, x_{w+1}]$

$$P_w(x) = a_w + b_w x + c_w x^2 + l\sqrt{c^2 - x^2},$$

When $c_o = 0$, we extract from $[0, x_1]$

$$P_0(x) = a_0 + b_0 x + c_0 x^2 + d_0 x^3 + l\sqrt{c^2 - x^2}$$

The comparable interferogram fringe shift $\delta(x)$; in every small interval external to the shock-wave $[x_j, x_{j+1}]\,(j = v, v+1, \cdots, N-1)$ we use the ternary or binary polynomial:

$$P_j(x) = a_j + b_j x + c_j x^2 + d_j x^3,$$
$$P_j(x) = a_j + b_j x + c_j x^2 \qquad (j = v, N-1)$$

as the comparable interferometric fringe shift $\delta(x)$. See [4]. By using again the value δ_k, we can state the various coefficients a_i, b_i, c_i. According to the conclusions obtained in section 3

$$\rho(r_j) - \rho_0 = -\frac{\lambda^*}{\pi K}\int_{r_j}^{R} \frac{\delta'(x)}{\sqrt{x^2 - r_j^2}}\,dx = -\frac{\lambda^*}{\pi K}\sum_{k=j}^{N-1}\int_{r_k}^{r_{k+1}} \frac{\delta'(x)}{\sqrt{x^2 - r_j^2}}\,dx.$$

By using $P'_i(x)$ as stated above to substitute $\delta'(x)$, we get:

$$\rho(r_j) - \rho_0 = -\frac{\lambda^*}{\pi K}\sum_{k=j}^{N-1}\int_{r_k}^{r_{k+1}} \frac{P'_k(x)}{\sqrt{x^2 - r_j^2}}\,dx.$$

After computation of each integral, we have the parallel systematization:

$$\rho(r_w) = \rho_0 + \frac{1}{R}\sum_{k=w}^{N-1} a_{w,k}\,\delta_k;$$

$$\rho(r_j) = \rho_0 + \frac{1}{R}\sum_{k=j-1}^{N-1} a_{j,k}\,\delta_k, \quad (j = w+1, w+2, \cdots, v-2, v, v+1, \cdots, N-1);$$ (9)

$$\rho(r_{v-1}) = \rho_0 + \frac{1}{R}\sum_{k=v-3}^{N-1} a_{v-1,k}\,\delta_k.$$

We will note:

$$C^* = \frac{\lambda^* N}{12\pi K},\quad B_1 = \sqrt{2v-1},\ B_2 = \sqrt{4v-1},\ B_3 = \sqrt{6v-9},\ B_4 = \sqrt{8v-16},$$
$$D = 3B_1 - 3B_2 + B_3,\ E = 2B_1 - B_2,\ F = 3B_1 - B_3,\ G = 3B_2 - 2B_3,\ H = B_1 - 2B_2 + B_3,$$
$$I = B_1 - 3B_2 + 3B_3 - B_4;\ F(j,k) = (6k^2 - 2 + 3j^2)\ln(k + \sqrt{k^2 - j^2}) - 9k\sqrt{k^2 - j^2},$$
$$T(j,k) = \operatorname{arctg}\sqrt{\frac{v^2-(k+1)^2}{(k+1)^2-j^2}} - \operatorname{arctg}\sqrt{\frac{v^2-k^2}{k^2-j^2}},$$
$$L(j) = \frac{v + \sqrt{v^2 - j^2}}{v - 2 + \sqrt{(v-2)^2 - j^2}},\qquad J(j) = \sqrt{v^2 - j^2} - \sqrt{(v-2)^2 - j^2};$$

$$A(0) = 2.375v - 2.5\sqrt{v^2-1} + 0.125\sqrt{v^2-1} - \arcsin\frac{1}{v} +$$
$$+ \frac{1}{12}(\sqrt{v^2-9} - 3\sqrt{v^2-4} + 3\sqrt{v^2-1} - v)\cdot F(0,1) -$$
$$- (0.5\sqrt{v^2-4} - 2\sqrt{v^2-1} + 1.5v)\cdot \ln 2 +$$
$$+ \sqrt{v^2-4} - 2\sqrt{v^2-1} + v + T(0,1) +$$
$$+ \sum_{k=2}^{v-3}\Big\{\frac{1}{12}(\sqrt{v^2-(k+2)^2} - 4\sqrt{v^2-(k+1)^2} + 6\sqrt{v^2-k^2} - 4\sqrt{v^2-(k-1)^2}$$
$$+ \sqrt{v^2-(k-2)^2})\cdot F(0,k) + T(0,k)\Big\} - \frac{1}{12}I\cdot F(0,v-2) +$$
$$+ \{(v-2.5)B_1 - 2(v-2)B_2 + (v-1.5)B_3\}\ln(2v-4) - H\cdot(v-2),$$
$$A(w) = -\{(w+0.5)\sqrt{v^2-(w+2)^2} - 2(w+1)\sqrt{v^2-(w+1)^2} +$$
$$+ (w+1.5)\sqrt{v^2-w^2}\}\ \ln w +$$
$$+ \frac{1}{12}\Big\{\sqrt{v^2-(w+3)^2} - 3\sqrt{v^2-(w+2)^2} + 3\sqrt{v^2-(w+1)^2} -$$
$$- \sqrt{v^2-w^2}\Big\}\cdot F(w,w+1) +$$
$$+ \operatorname{arctg}\sqrt{\frac{v^2-(w+2)^2}{4w+4}} - \frac{\pi}{2} +$$
$$+ \sum_{k=w+2}^{v-3}\Big\{\frac{1}{12}\Big(\sqrt{v^2-(k+2)^2} - 4\sqrt{v^2-(k+1)^2} + 6\sqrt{v^2-k^2} -$$
$$- 4\sqrt{v^2-(k-1)^2} + \sqrt{v^2-(k-2)^2}\Big)\cdot F(w,k) + T(w,k)\Big\} -$$
$$- \frac{1}{12}I\cdot F(w,v-2) + \{(v-2.5)B_1 - 2(v-2)B_2 + (v-1.5)B_3\}\cdot$$
$$\cdot \ln(v - 2 + \sqrt{(v-2)^2 - w^2}) - H\cdot\sqrt{(v-2)^2 - w^2},\qquad (w \geq 1),$$

$$
\begin{aligned}
A(j) = & -\{(j-0.5)\sqrt{v^2-(j+1)^2} - 2j\sqrt{v^2-j^2} + (j+0.5)\sqrt{v^2-(j-1)^2}\}\ln j + \\
& + \frac{1}{12}\Big\{\sqrt{v^2-(j+2)^2} - 3\sqrt{v^2-(j+1)^2} + 3\sqrt{v^2-j^2} - \\
& - \sqrt{v^2-(j-1)^2}\Big\} F(j,j) + \operatorname{arctg}\sqrt{\frac{v^2-(j+1)^2}{2j+1}} - \frac{\pi}{2} + \\
& + \sum_{k=j+1}^{v-3}\Big\{\frac{1}{12}\Big(\sqrt{v^2-(k+2)^2} - 4\sqrt{v^2-(k+1)^2} + 6\sqrt{v^2-k^2} - \\
& - 4\sqrt{v^2-(k-1)^2} + \sqrt{v^2-(k-2)^2}\Big)\cdot F(j,k) + T(j,k)\Big\} - \\
& - \frac{1}{12} I\cdot F(j,v-2) + \Big\{(v-2.5)B_1 - 2(v-2)B_2 + \\
& + (v-1.5)B_3\Big\}\ln\left(v-2+\sqrt{(v-2)^2-j^2}\right) - H\cdot\sqrt{(v-2)^2-j^2}\,.
\end{aligned}
$$

$$(j = w+1, w+2, \cdots, v-3).$$

Each coefficient $a_{i,k}$ in the formula of the transformation (9), is expressed below (supposing $w+5<v<N-5$)

$$
a_{w,w} = \begin{cases} 12C^{*}\left\{1.125 + \frac{11}{6}\ln 2\right\} & \text{when } w=0 \\ C^{*}\{F(w,w+2) - F(w,w+1) - 6(2w+3)\ln w\} & \text{when } w\geqslant 1 \end{cases}
$$

$$
a_{w,w+1} = \begin{cases} 12C^{*}\left\{-1.5 + \frac{13}{3}\ln 3 - \frac{22}{3}\ln 2\right\} & \text{when } w=0 \\ C^{*}\{F(w,w+3) - 4F(w,w+2) + 3F(w,w+1) + 24(w+1)\ln w\} & \text{when } w\geqslant 1 \end{cases}
$$

$$
a_{w,w+2} = \begin{cases} 12C^{*}\left\{0.375 - \frac{52}{3}\ln 3 + \frac{80}{3}\ln 2\right\} & \text{when } w=0 \\ C^{*}\{F(w,w+4) - 4F(w,w+3) + 6F(w,w+2) - 3F(w,w+1) - \\ \quad - 6(2w+1)\ln w\} & \text{when } w\geqslant 1 \end{cases}
$$

$$a_{j,k} = C^{*}\{F(j,k+2) - 4F(j,k+1) + 6F(j,k) - 4F(j,k-1) + F(j,k-2)\},$$

$$(j=w,\ k=w+3, w+4, \cdots, v-4);$$

$$(j=w+1, w+2, \cdots, v-6,\ k=j+2, j+3, \cdots, v-4);$$

$$(j=w, w+1, \cdots, v+1,\ k=v+3, v+4, \cdots, N-3);$$

$$(j=v+2, v+3, \cdots, N-5,\ k=j+2, j+3, \cdots, N-3);$$

$$a_{j,j-1} = C^{*}\{F(j,j+1) - F(j,j) - 6(2j+1)\ln j\},$$

$$(j=w+1, w+2, \cdots, v-3, v+1, v+2, \cdots, N-2);$$

$$a_{j,j} = C^{*}\{F(j,j+2) - 4F(j,j+1) + 3F(j,j) + 24j\ln j\},$$

$$(j=w+1, w+2, \cdots, v-4, v+1, v+2, \cdots, N-3);$$

$$a_{j,j+1} = C^{*}\{F(j,j+3) - 4F(j,j+2) + 6F(j,j+1) - 3F(j,j) - 6(2j-1)\ln j\},$$

$$(j=w+1, w+2, \cdots, v-5, v+1, v+2, \cdots, N-4);$$

$$
\begin{aligned}
a_{j,v-3} = & C^{*}\{F(j,v-5) - 4F(j,v-4) + 6F(j,v-3) - 3F(j,v-2) + \\
& + 6(2v-3)\ln\left(v-2+\sqrt{(v-2)^2-j^2}\right) - 12\sqrt{(v-2)^2-j^2}\} - \\
& - \frac{12C^{*}}{D}\left\{\left(1-\frac{B_1E}{2}\right)B_1L(j) + E\cdot J(j) + A(j) - \operatorname{arctg}\frac{B_2}{\sqrt{(v-2)^2-j^2}}\right\}.
\end{aligned}
$$

$$(j=w, w+1, \cdots, v-5);$$

$$a_{j,v-2}=C^{*}\{F(j,v-4)-4F(j,v-3)+3F(j,v-2)-24(v-2)\times\ln\cdot(v-2+\sqrt{(v-2)^2-j^2})+24\sqrt{(v-2)^2-j^2}\}-\frac{12C^{*}}{D}\Big\{\Big(-3+\frac{B_1F}{2}\Big)B_1L(j)-F\cdot J(j)-3A(j)+3\,\mathrm{arctg}\frac{B_2}{\sqrt{(v-2)^2-j^2}}\Big\},$$

$$(j=w,w+1,\cdots,v-4);$$

$$a_{j,v-1}=C^{*}\{F(j,v-3)-F(j,v-2)+6(2v-5)\ln(v-2+\sqrt{(v-2)^2-j^2})-12\sqrt{(v-2)^2-j^2}\}-\frac{12C^{*}}{D}\Big\{\Big(-D+3B_1-\frac{B_1^2}{2}G\Big)\cdot L(j)+G\cdot J(j)+3A(j)-3\,\mathrm{arctg}\frac{B_2}{\sqrt{(v-2)^2-j^2}}\Big\},\quad(j=w,w+1,\cdots,v-3);$$

$$a_{j,v}=C^{*}\{F(j,v+2)-F(j,v+1)-6(2v+3)\ln(v+\sqrt{v^2-j^2})+12\sqrt{v^2-j^2}\}-\frac{12C^{*}}{D}\Big\{\Big(D-B_1-\frac{B_1^2}{2}H\Big)\cdot L(j)+H\cdot J(j)-A(j)+\mathrm{arctg}\frac{B_2}{\sqrt{(v-2)^2-j^2}}\Big\},$$

$$(j=w,w+1,\cdots,v-3);$$

$$a_{v-4,v-3}=C^{*}\{-3F(v-4,v-4)+6F(v-4,v-3)-3F(v-4,v-2)-6(2v-9)\ln(v-4)+6(2v-3)\ln(v-2+2\sqrt{v-3})-24\sqrt{v-3}\}-\frac{12C^{*}}{D}\Big\{\Big(1-\frac{B_1\cdot E}{2}\Big)B_1\cdot L(v-4)+E\cdot J(v-4)+A(v-4)-\mathrm{arctg}\frac{B_2}{2\sqrt{v-3}}\Big\};$$

$$a_{v-3,v-3}=C^{*}\{3F(v-3,v-3)-3F(v-3,v-2)+6(2v-3)\ln(v-2+\sqrt{2v-5})-12\sqrt{2v-5}+24(v-3)\ln(v-3)\}-\frac{12C^{*}}{D}\Big\{\Big(1-\frac{B_1\cdot E}{2}\Big)B_1\cdot L(v-3)+E\cdot J(v-3)+A(v-3)-\mathrm{arctg}\frac{B_2}{\sqrt{2v-5}}\Big\};$$

$$a_{v-3,v-2}=C^{*}\{3F(v-3,v-2)-3F(v-3,v-3)-6(2v-7)\ln(v-3)-24(v-2)\ln(v-2+\sqrt{2v-5})+24\sqrt{2v-5}\}-\frac{12C^{*}}{D}\Big\{\Big(-3+\frac{B_1\cdot F}{2}\Big)B_1\cdot L(v-3)-F\cdot J(v-3)-3A(v-3)+3\,\mathrm{arctg}\frac{B_2}{\sqrt{2v-5}}\Big\};$$

$$a_{v-2,v-3}=\frac{12C^{*}}{D}\Big\{\frac{\pi}{2}-B_2\cdot E-\Big(1-\frac{B_1\cdot E}{2}\Big)\cdot B_1\cdot\ln\frac{v+B_2}{v-2}\Big\};$$

$$a_{v-2,v-2}=\frac{12C^{*}}{D}\Big\{-\frac{3}{2}\pi+B_2(3E-D)+\Big[3-\frac{B_1}{2}(3E-D)\Big]B_1\cdot\ln\frac{v+B_2}{v-2}\Big\};$$

$$a_{v-2,v-1}=\frac{12C^{*}}{D}\Big\{\frac{3}{2}\pi-B_2(3E-2D)+\Big[D-3B_1+\frac{B_1^2}{2}(3E-2D)\Big]\ln\frac{v+B_2}{v-2}\Big\};$$

$$a_{v-2,v}=\frac{12C^{*}}{D}\Big\{-\frac{\pi}{2}+B_2\cdot E-\Big[D-B_1+\frac{B_1^2}{2}(E-D)\Big]\ln\frac{v+B_2}{v-2}\Big\}+C^{*}\{F(v-2,v+2)-F(v-2,v+1)-6(2v+3)\ln(v+B_2)\};$$

$$a_{v-1,v-3}=\frac{12C^{*}}{D}\Big\{\frac{\pi}{2}-B_1\cdot E-\Big(1-\frac{B_1\cdot E}{2}\Big)B_1\cdot\ln\frac{v+B_1}{v-1}\Big\};$$

$$a_{v-1,v-2} = \frac{12C^*}{D}\left\{-\frac{3}{2}\pi + B_1(3E-D) + \left[3-\frac{B_1}{2}(3E-D)\right]B_1 \cdot \ln\frac{v+B_1}{v-1}\right\};$$

$$a_{v-1,v-1} = \frac{12C^*}{D}\left\{\frac{3}{2}\pi - B_1(3E-2D) + \left[D-3B_1+\frac{B_1^2}{2}(3E-2D)\right]\ln\frac{v+B_1}{v-1}\right\};$$

$$a_{v-1,v} = \frac{12C^*}{D}\left\{-\frac{\pi}{2} + B_1 \cdot E - \left[D-B_1+\frac{B_1^2}{2}(E-D)\right]\ln\frac{v+B_1}{v-1}\right\} +$$
$$+ C^*\{F(v-1,v+2) - F(v-1,v+1) - 6(2v+3)\ln(v+B_1)\};$$

$$a_{j,v+1} = C^*\{F(j,v+3) - 4F(j,v+2) + 3F(j,v+1) - 24\sqrt{v^2-j^2} +$$
$$+ 24(v+1)\ln(v+\sqrt{v^2-j^2}), \qquad (j = w, w+1, \cdots, v);$$

$$a_{j,v+2} = C^*\{F(j,v+4) - 4F(j,v+3) + 6F(j,v+2) - 3F(j,v+1) + 12\sqrt{v^2-j^2} -$$
$$- 6(2v+1)\ln(v+\sqrt{v^2-j^2})\}, \qquad (j = w, w+1, \cdots, v);$$

$$a_{v,v-1} = 0;$$

$$a_{v,v} = C^*\{-F(v,v+1) + F(v,v+2) - 6(2v+3)\ln v\};$$

$$a_{j,N-2} = C^*\{F(j,N-4) - 4F(j,N-3) + 6F(j,N-2) - 3F(j,N-1) +$$
$$+ 6(2N-1)\ln(N+\sqrt{N^2-j^2}) - 12\sqrt{N^2-j^2}\} \qquad (j = w, w+1, \cdots, N-4);$$

$$a_{j,N-1} = C^*\{F(j,N-3) - 4F(j,N-2) + 3F(j,N-1) -$$
$$- 24(N-1)\ln(N+\sqrt{N^2-j^2}) + 24\sqrt{N^2-j^2}\} \quad (j = w, w+1, \cdots, N-3);$$

$$a_{N-3,N-2} = C^*\{-3F(N-3,N-3) + 6F(N-3,N-2) - 3F(N-3,N-1) -$$
$$- 6(2N-7)\ln(N-3) + 6(2N-1)\ln(N+\sqrt{6N-9}) - 12\sqrt{6N-9}\};$$

$$a_{N-2,N-2} = C^*\{3F(N-2,N-2) - 3F(N-2,N-1) + 6(2N-1)\ln(N+2\sqrt{N-1})$$
$$- 24\sqrt{N-1} + 24(N-2)\ln(N-2)\};$$

$$a_{N-2,N-1} = C^*\{3F(N-2,N-1) - 3F(N-2,N-2) - 24(N-1) \cdot$$
$$\cdot \ln(N+2\sqrt{N-1}) + 48\sqrt{N-1} - 6(2N-5)\ln(N-2)\};$$

$$a_{N-1,N-2} = C^*\left\{6(2N-1)\ln\frac{N+\sqrt{2N-1}}{N-1} - 12\sqrt{2N-1}\right\};$$

$$a_{N-1,N-1} = C^*\left\{-24(N-1)\ln\frac{N+\sqrt{2N-1}}{N-1} + 24\sqrt{2N-1}\right\}.$$

According to conclusion 2 obtained in section II, and Eq. (7), it is possible to establish the approximate rebound equality for the density of the shock-wave.

$$\rho(c_-) - \rho(c_+) = \lambda^* l/2K, \qquad (10)$$

in which l is computed as in (8). Especially when r≥c, and in the case when $\rho(r)-\rho_c=0$

$$\rho(c_-) - \rho_0 = \lambda^* l/2K. \qquad (11)$$

Supposing the measurements of the interferometric fringe shift give the following readings:

$$\delta(x) = \begin{cases} f(x) + l\sqrt{c^2 - x^2}, & 当 c_0 \leqslant x < c 时, \\ f(x) & 当 c \leqslant x \leqslant R 时. \end{cases}$$

and if in addition f'(x) is continuous with $[c_0,R]$ and f''(x) a fractionate succession, we have proven (in a further study on the computation of errors) by the above calculation of the density of the airflow $\rho(r_i)$, the existence of an error such as:

$$|\triangle\rho(r_i)| \leqslant \frac{\lambda^*}{\pi K} M h^{1-\sigma}. \qquad (12)$$

in which the constant M and c, R and $\max_{c_0 \leq x \leq R} |f''(x)|$ are related, and the positive number σ equivalent to the wave h, being extremely small, can be arbitrarily small.

$$|\triangle(\rho(c_-) - \rho(c_+))| \leqslant \frac{\lambda^*}{\pi K} M' \max_{x_2 - 2 \leq x_1, x_2 \leq c} |f''(x_1) - f''(x_2)| h^{\frac{1}{2}}. \qquad (13)$$

The constant M' and c are related. From computation in (13) it is obvious that the approximate calculation (10) is rather precise.
From Table 9 established in [2] regarding the interferograms of spherical projectiles, we have estimated the values of δ(x,z), the interferometric fringe shift, and used them in the computation with the method described above. Fig. 3 shows the isograph of the comparative density values ρ/ρ_0 inside the shock-wave. Fig. 4 is the reproduction of Fig. 10 borrowed from [2]. Table 1 gives the concentration saltatory values of the shock-wave

between I and V, as well as the density measurements inside the shock-wave $\rho-\rho_0$. It is apparent that our method is simple and practical.

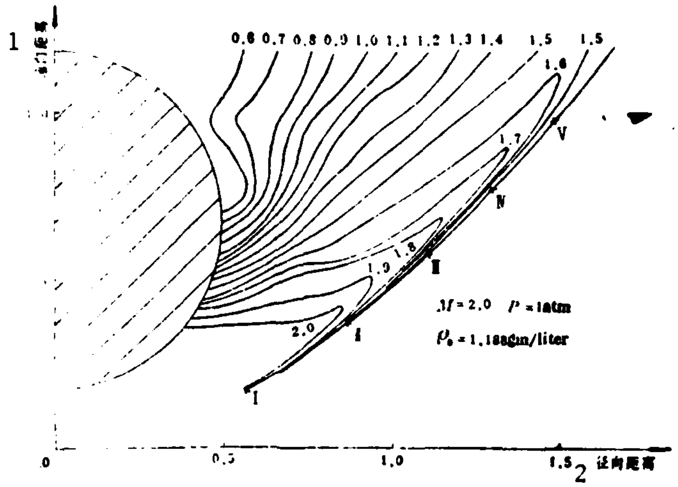

Fig. 3. *Density ratio within the shock-waves* $\rho(r)/\rho_0$

Key: (1) axial distance; (2) radial distance

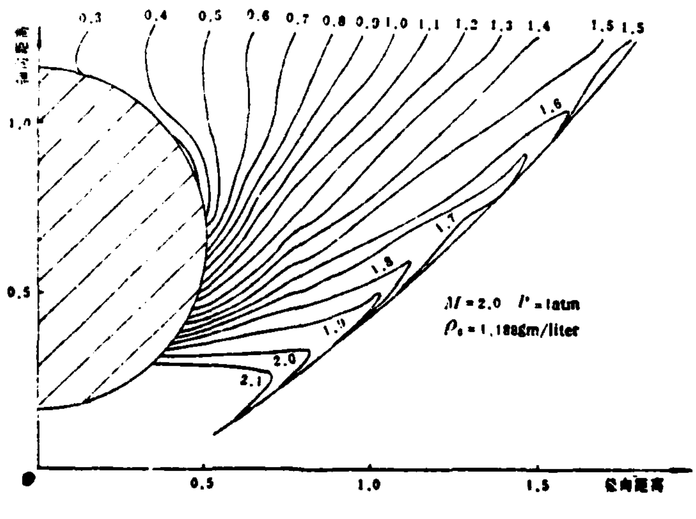

Fig. 4. Density ratio within the shock-waves $\rho(r)/\rho_0$ [2]

Key: (1) axial distance; (2) radial distance

Table 1.

	I	II	III	IV	V
$\rho_- - \rho_0$	0.61	0.41	0.26	0.19	0.14
ρ_-	1.60	1.60	1.44	1.38	1.33

IV. CASE OF SEVERAL SHOCK-WAVES

When a point headed cylindrical supersonic projectile is in flight, two or more shock-waves can be observed. As illustrated in Fig. 1, cross sections 2-2 and 3-3 correspond respectively to two or three shock-waves.

With two shock-waves as an example, supposing that the wave originates outside r-c_1 and r=c_2, the projectiles' cross-sectional radius is c_0:

$$c_0 < c_1 < c_2,$$

we extract the isometric partition;

$$c_0 = x_w < x_{w+1} < x_{w+2} < \cdots < x_{v_1} = c_1 < x_{v_1+1} < x_{v_1+2} < \cdots < x_{v_2} = c_2.$$

In the expression $[x_j, x_{j+1}]$ $(j = w, w+1, \cdots, v_1 - 1)$ we extract the binary or ternary polynomial comparable $\delta(x)$ with the additional term $l_1\sqrt{c_1^2 - x^2}$. In the expression $[x_j, x_{j+1}]$ $(j = v_1, v_1 + 1, \cdots, v_2 - 1)$ we extract the binary or ternary polynomial comparable $\delta(x)$ with additional term $l_2\sqrt{c_2^2 - x^2}$. By repeating the process described in section III, we can definitely extract l_1, l_2 and the coefficients of each polynomial, introducing them in

$$\rho(r_j) - \rho_0 = -\frac{\lambda^b}{\pi K}\int_{r_j}^{c_2} \frac{\delta'(x)}{\sqrt{x^2 - r_j^2}} dx, \quad (j = w, w+1, \cdots, v_2 - 1)$$

which gives us the parallel systematization:

$$\rho(r_w) = \rho_0 + \sum_{k=w}^{v_2-1} a_{w,k}\,\delta_k;$$

$$\rho(r_j) = \rho_0 + \sum_{k=j-1}^{v_2-1} a_{j,k}\,\delta_k, \quad (j = w+1, \cdots, v_1-2, v_1+1, \cdots, v_2-2);$$

$$\rho(r_{v_1}) = \rho_0 + \sum_{k=v_1}^{v_2-1} a_{v_1,k}\,\delta_k;$$

$$\rho(r_i) = \rho_0 + \sum_{k=i-2}^{v_2-1} a_{i,k}\,\delta_k, \quad (i = v_1-1, v_2-1).$$

in which each equality of transformation coefficient $a_{k,k}$ is comparable to the derivation of section III.

On the external shock-wave c_2, the concentration saltatory value is:

$$\rho(c_{2-}) - \rho_0 = \lambda^* l_2/2K.$$

On the internal side of wave c_2, the value is:

$$\rho(c_{2-}) = \rho_0 + \lambda^* l_2/2K,$$

in which:

$$l_2 = \frac{1}{D_2 h}\left(-\delta_{v_2} + 3\delta_{v_2-1} - 3\delta_{v_2-2} + \delta_{v_2-3}\right),$$

$$D_2 = 3\sqrt{2v_2-1} - 3\sqrt{4v_2-1} + \sqrt{6v_2-9};$$

On the internal side of shock-wave c_1, from the concentration saltatory values

$$\rho(c_{1-}) - \rho(c_{1+}) = \lambda^* l_1/2K$$

and

$$\rho(c_{1+}) = \rho_0 + \sum_{k=v_1}^{v_2-1} a_{v_1,k}\,\delta_k$$

we obtain the concentration rebound values of the internal side of the shock-wave:

$$\rho(c_{1-}) = \frac{\lambda^* l_1}{2K} + \rho_0 + \sum_{k=v_1}^{v_2-1} a_{v_1,k}\,\delta_k.$$

in which:

$$l_1 = \frac{1}{D_1 h}\left(-\delta_{v_1} + 3\delta_{v_1-1} - 3\delta_{v_1-2} + \delta_{v_1-3}\right),$$

$$D_1 = 3\sqrt{2v_1-1} - 3\sqrt{4v_1-1} + \sqrt{6v_1-9}.$$

V. PLAN FOR A SIMPLIFIED COMPUTATION

We take as an example the case of two shock-waves. The partition is:

$$c_0 = x_w < x_{w+1} < \cdots < x_{v_1} = c_1 < x_{v_1+1} < \cdots < x_{v_2} = c_2 < x_{v_2+1} < \cdots \quad x_N = R.$$

Previously we only considered one shock-wave c_2. As in Eq. (9) in section III, we extract $v=v_2$, $w=v_1$, to compute the value of the concentration

$$\rho(r_{w+1}),\ \cdots,\ \rho(r_{v-1})$$

We distinguish the values of concentration of the shock-waves c_1 and c_2.

$$\rho(r_{v_1+1}),\ \cdots,\ \rho(r_{v_2-1}).$$

The rebound value of the airflow concentration of the shock-wave c_2 is:

$$\rho(c_{2-}) - \rho_0 = \lambda^* l_2/2K,$$

in which l_2 is similar to section IV. Secondly, we will review the case of one shock-wave c_1. Again according to Eq. (9), we extract $v=v_1$, $N=v_2$, to compute the concentration value:

$$\rho(r_w),\ \cdots,\ \rho(r_{v-1}),\ \rho(r_v)$$

We distinguish the concentration values in the shock-wave c_1 and outside of it:

$$\rho(r_w),\ \cdots,\ \rho(r_{v_1-1}),\ \rho(c_{1+}).$$

The airflow concentration values are:

$$\rho(c_{1-}) - \rho(c_{1+}) = \lambda^* l_1/2K,$$

in which l is similar to the value obtained in section IV.

The method described above can repeatedly be applied to the case of several shock-waves.

[1] Ding Peizhu, Pan Shoufu, Abel transformation of plasma spectra involving shock waves reported at the "All-China conference on High Energy Density Dynamics Testing Technology", Changsha, June 1980.

[2] Bennett, F. D. *et al.*, *J. Appl. Phys.*, 23, 453 (1952).

[3] Ladenberg, R. D., Physical Measurements in Gas Dynamic and Combustion, Oxford University Press, 1955.

[4] Bockasten, K., *JOSA*, 51, 943 (1961).

Abstract

The method of numerical solution on four physical conclusions and "The Abel Transformation of Plasma Spectroscopy Involved Shock Wave" obtained by the same authors in [1] is extended to Mach-Zehnder *interferogram* analysis of supersonic airflow about cylindrical symmetric projectiles. Three similar physical conclusions about the relation between the interferometric fringe shift, $\delta(x,z)$, measured from M-Z inferferogram and the density difference, $\rho(r,z)-\rho_0$, at each point in the supersonic airflow feild are obtained, and all transformation coefficient formulas used to calculate the density difference, $\rho(r,z)-\rho_0$, according to the interferometric fringe shift, $\delta(x,z)$, have been given. As an example, by use of experimental data given in [2], airflow field of cylindrical symmetric projectiles is calculated and the better results have been obtained. A simplied calculation method which deals with many shock waves existing in airflow feild has been given.

DATE

FILMED

7-8